IOPscience iopscience.iop.org

Home Search Collections Journals About Contact us My IOPscience

Satellite observation of tropical forest seasonality: spatial patterns of carbon exchange in Amazonia

This content has been downloaded from IOPscience. Please scroll down to see the full text.

2015 Environ. Res. Lett. 10 084005

(http://iopscience.iop.org/1748-9326/10/8/084005)

View the table of contents for this issue, or go to the journal homepage for more

Download details:

IP Address: 210.77.64.109
This content was downloaded on 13/04/2017 at 06:24

Please note that terms and conditions apply.

You may also be interested in:

Sunlight mediated seasonality in canopy structure and photosynthetic activity of Amazonian rainforests
Jian Bi, Yuri Knyazikhin, Sungho Choi et al.

Asynchronous Amazon forest canopy phenology indicates adaptation to both water and light availability
Matthew O Jones, John S Kimball and Ramakrishna R Nemani

Estimation of aboveground net primary productivity in secondary tropical dry forests using the Carnegie–Ames–Stanford Approach (CASA) model
S Cao, GA Sanchez-Azofeifa, SM Duran et al.

Mulga, a major tropical dry open forest of Australia: recent insights to carbon and water fluxes
Derek Eamus, Alfredo Huete, James Cleverly et al.

Potential hydrologic changes in the Amazon by the end of the 21st century and the groundwater buffer
Yadu N Pokhrel, Ying Fan and Gonzalo Miguez-Macho

Linking primary production, climate and land use along an urban–wildland transect: asatellite view
Yonghong Hu, Gensuo Jia and Huadong Guo

Intrinsic climate dependency of ecosystem light and water-use-efficiencies across Australian biomes
Hao Shi, Longhui Li, Derek Eamus et al.

Large-scale heterogeneity of Amazonian phenology revealed from 26-year long AVHRR/NDVI time-series
Fabrício B Silva, Yosio E Shimabukuro, Luiz E O C Aragão et al.

Environmental Research Letters

LETTER

Satellite observation of tropical forest seasonality: spatial patterns of carbon exchange in Amazonia

Liang Xu[1,4], **Sassan S Saatchi**[1,2,4], **Yan Yang**[1,3], **Ranga B Myneni**[3], **Christian Frankenberg**[2], **Diya Chowdhury**[1] **and Jian Bi**[3]

[1] Institute of the Environment and Sustainability, University of California, Los Angeles, CA 90095, USA
[2] Jet Propulsion Laboratory, California Institute of Technology, Pasadena, CA 91109, USA
[3] Department of Earth and Environment, Boston University, Boston, MA 02215, USA
[4] Author for correspondence.

E-mail: xuliang@ucla.edu **and** saatchi@jpl.nasa.gov

OPEN ACCESS

RECEIVED
23 October 2014

REVISED
11 June 2015

ACCEPTED FOR PUBLICATION
4 July 2015

PUBLISHED
3 August 2015

Content from this work may be used under the terms of the Creative Commons Attribution 3.0 licence.

Any further distribution of this work must maintain attribution to the author(s) and the title of the work, journal citation and DOI.

Keywords: vegetation seasonality, amazonia, tropical forest, remote sensing, pheno-region, GPP, fluorescence

Supplementary material for this article is available online

Abstract

Determining the seasonality of terrestrial carbon exchange with the atmosphere remains a challenge in tropical forests because of the heterogeneity of ecosystem and climate. The magnitude and spatial variability of this flux are unknown, particularly in Amazonia where empirical upscaling approaches from spatially sparse *in situ* measurements and simulations from process-based models have been challenged in recent scientific literature. Here, we use satellite proxy observations of canopy structure, skin temperature, water content, and optical properties over a period of 10 years (2000–2009) to constrain and quantify the spatial pattern and seasonality of carbon exchange of Amazonian forests. We identify nine regions through an optimized cluster approach with distinct leaf phenology synchronized with either water or light availability and corresponding seasonal cycles of gross primary production (GPP), covering more than 600 million ha of remaining old growth forests of Amazonia. We find South and Southwestern regions show strong seasonality of GPP with a peak in the wet season; while from Central Western to Northeastern Amazonia cover three regions with rising GPP in the dry season. The remaining four regions have significant but weak seasonality. These patterns agree with satellite florescence observations, a better proxy for photosynthetic activity. Our results suggest that only one-third of the patterns can be explained by the spatial autocorrelation caused by intra-annual variability of climate over Amazonia. The remaining two-thirds of variations are due to biogeography of the Amazon basin driven by forest composition, structure, and nutrients. These patterns, for the first time, provide a complex picture of seasonal changes of tropical forests related to photosynthesis and influenced by water, light, and stomatal responses of trees that can improve modeling of regional carbon cycle and future prediction of impacts of climate change.

Introduction

The terrestrial gross primary production (GPP) is considered the largest CO_2 flux (123 ± 8 petagrams) and responsible for driving several ecosystem functions globally (Beer *et al* 2010). Estimates of magnitude and regional variations of this flux remain uncertain in humid tropical forests, particularly in Amazonia (Huntingford *et al* 2013, Schimel *et al* 2014) where limited ground data have caused gross assumptions about seasonality and heterogeneity of these forests (Clark 2004). Forests of Amazonia, although considered evergreen, appear to have seasonal cycles, following the rhythms of rainfall and radiation (Myneni *et al* 2007, Fu *et al* 2013) that significantly impact their carbon assimilation and GPP (Clark 2004, Lee *et al* 2013, Fischer *et al* 2014). Experimental studies and ecosystem modeling suggest that availability of

© 2015 IOP Publishing Ltd

water and light regulate carbon assimilation of the Amazon forests (Saleska *et al* 2003, Baker *et al* 2008, Kim *et al* 2012). Eddy covariance measurements in Central Amazonia indicate that there is an increased net ecosystem productivity and evapotranspiration during dry season that may suggest the greening of canopy or emergence of new leaves (Hutyra *et al* 2007, Restrepo-Coupe *et al* 2013). However, ground observations in Southern and Southwest Amazon support more of a distinct dry season decline in canopy photosynthesis due to water stress (Vourlitis *et al* 2005, Saleska *et al* 2009, Restrepo-Coupe *et al* 2013, Araujo-Murakami *et al* 2014, Malhi *et al* 2014, Rowland *et al* 2014).

This diversity in results point to a significant heterogeneity in vegetation interaction with climate, creating spatially variable seasonality of GPP that cannot be resolved at landscape to regional scales with limited ground and tower flux data (Restrepo-Coupe *et al* 2013). In general, GPP is not directly observed at the plot or tower flux sites but approximately estimated from either observations of net primary production (NPP) and autotrophic respiration (R_a) as $GPP = NPP + R_a$ from detailed plot level measurements (Doughty *et al* 2014) or derived from tower eddy covariance measurements of the net ecosystem exchange. In either case, the uncertainty in GPP estimation is high and is strongly impacted by the accuracy of ground measurements (Malhi *et al* 2009) and various sources of errors in tower observations (Restrepo-Coupe *et al* 2013). Given the lack of reliable direct *in situ* measurements of GPP and the potential heterogeneity of GPP at the landscape scale, making the few plot or tower based estimates sparse and inadequate (Restrepo-Coupe *et al* 2013, Malhi *et al* 2014), consequently, spatially refined estimates of GPP are often derived from remote sensing products or a combination of ecosystem models, climate, and remote sensing observations. The use of various satellite measurements directly related to vegetation biophysical parameters, such as the leaf area index, fraction of absorbed photosynthetically active radiation (fPAR), or vegetation greenness indices like the normalized difference vegetation index (NDVI) (Hashimoto *et al* 2012) are key variables to examine the variations and seasonality in GPP related to vegetation productivity and photosynthetic activities.

Studies using optical satellite data and vegetation indices have shown that the signals related to vegetation photosynthesis increase during the light-rich dry season in Amazonia (Myneni *et al* 2007, Samanta *et al* 2012), suggesting the seasonality of photosynthesis is driven by the light-controlled leaf phenology through the root water dynamics or under no water stress (Kim *et al* 2012). However, the observed seasonal 'green-up' (Huete *et al* 2006, Myneni *et al* 2007) has been challenged in recent studies using estimates from satellite fluorescence sensors (Lee *et al* 2013), and also modeling effort showing sun-sensor geometry effects (Morton *et al* 2014). The multi-year analyses of these data have also shown that optical satellite observations in the tropics suffer from atmospheric contamination (Samanta *et al* 2010, Maeda *et al* 2014). These conflicting results point to the need for a comprehensive interpretation of satellite and ground observations for capturing regional variations of vegetation phenology and productivity. Current efforts on examining and mapping the spatial patterns of forest seasonality have been focused on either the non-tropical regions (White *et al* 2005), or the signal processing of multi-temporal observations from a single satellite-derived variable, such as NDVI (Silva *et al* 2013, Hilker *et al* 2014). But the use of green index alone is often not sufficient to capture the GPP changes in view of the modeling approaches such as the light-use-efficiency (LUE) model (Monteith 1972, Running *et al* 2004) or the water-use-efficiency model (Beer *et al* 2007, 2010).

Here, we quantify the spatial patterns of seasonality of the Amazonian forests by combining 3 long-term satellite observations over a decade (from 2000 to 2009). First, we use land surface temperature (LST) (Wan 2008) aboard Moderate Resolution Imaging Spectroradiometer (MODIS) as an approximate measure of the canopy skin temperature and a key control on photosynthetic activity and GPP (Sims *et al* 2008). LST is strongly correlated with PAR and vapor pressure deficit (VPD) (Sims *et al* 2008), both of which are essential for quantifying GPP spatial variations and seasonality. Second, we use microwave radar backscatter aboard QuikSCAT (QSCAT) as a proxy for canopy water content and VPD—a variable controlling the photosynthetic activity, which can be monitored all time irrespective of the presence of clouds, aerosols, or seasonality of incoming radiation (Frolking *et al* 2011, Saatchi *et al* 2013). And third, we included the Nadir BRDF (bidirectional reflectance distribution function) adjusted reflectance (NBAR) of near-infrared (NIR) band (Schaaf *et al* 2002, 2011) from MODIS satellite, as the proxy for illuminated canopy structure without the influence of sensor geometry (Knyazikhin *et al* 2013; SI discussion), a variable related to the FPAR seasonality and LUE used in GPP estimation (Monteith 1972). After careful quality checks, we expect that the average seasonality observed from the three different satellite proxy measurements over 10 years can reasonably delineate the spatial patterns of forest seasonality, and separate the forests of Amazonia into dominant phenological regions. The detected patterns are important for understanding the carbon exchange and the gross primary productivity (GPP) of Amazonia and may inspire future regional studies and *in situ* observations.

Methods

We used multiple satellite-derived products in this study, including greenness data—NDVI and

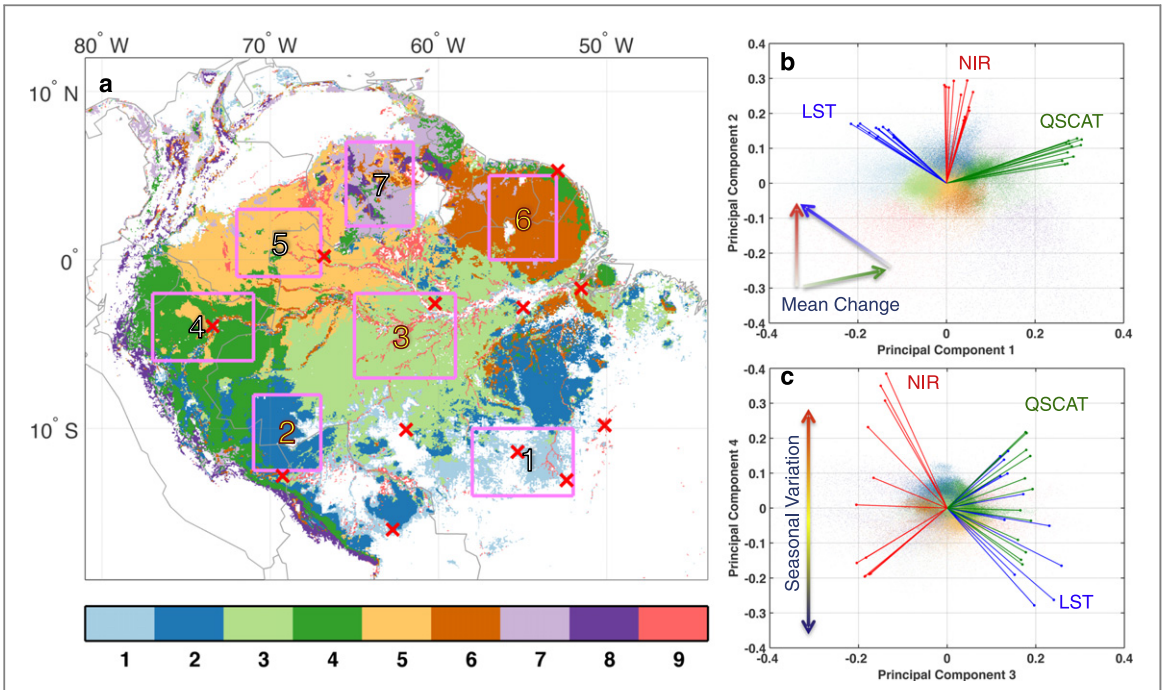

Figure 1. Seasonality cluster map of Amazonia. (a) Map of nine clusters using the *K*-Means clustering from the average monthly climatology data of LST, QSCAT, and NIR; (b) visualization of the cluster result in principal component (PC) domain (PC1 and PC2); (c) visualization of the cluster result in PC3 and PC4 domain (SI materials and methods). Colored region is classified as the Evergreen Broadleaf Forests (EBF) according to the latest MODIS land cover map. The boxes on the left panel were selected for regional studies (e.g. figure 2). Numbers in red color of panel (a) are selected regions for further discussion in the main text. Red cross signs denote the field sites available to validate our results (table S2; SI discussion). The direction and length of the vector in panels (b) and (c) indicate how each variable contributes to the two PC components. Each variable (LST, QSCAT and NIR) has 12 such vectors representing monthly climatology from January to December.

enhanced vegetation index, QSCAT radar measurements, LST and NBAR products from MODIS, sun-induced chlorophyll fluorescence (SIF) data from Greenhouse gases Observing SATellite (GOSAT), rainfall estimation from the Tropical Rainfall Measuring Mission (TRMM) product, and downward surface shortwave radiation from the Clouds and the Earth's Radiant Energy System (CERES) (SI materials and methods). The latest MODIS land cover product was used to define the research area and only pixels identified as evergreen broadleaf forests were selected to perform further analysis of seasonality in Amazonia. To evaluate the impact of observed satellite signals on the GPP estimation, we used the upscaled GPP from Max-Planck-Institute for Biogeochemistry (MPI-BGC) (Jung *et al* 2011) as a reference data set. The upscaled GPP has been developed by using the global network of tower flux measurements to reduce the uncertainty predicting regional variations along climate gradients, even in regions with limited tower measurements as in Amazonia. However, we consider the MPI-BGC GPP data may still have an uncertainty associated with individual grid cell, but using the data to examine seasonal variations at large regional scales could reduce the uncertainty by spatial filtering or averaging.

We made use of TIMESAT algorithm (Jönsson and Eklundh 2002, 2004, Eklundh and Jönsson 2011) to fill data gaps, smooth the signals and find seasonality parameters. The monthly climatology averaged from the decade of 2000s (2000–2009) was used as the input to obtain seasonality parameters. The *K*-means clustering algorithm was performed to create cluster maps from LST, NIR, and QSCAT. Sensitivity analyses using Random Forest (RF) machine learning algorithm (Breiman 2001) and multiple linear regression were performed to identify the important remote sensing variables for GPP prediction. For the regional GPP prediction, we used the RF model to develop a relationship between MPI-BGC GPP and LST, NIR and QSCAT data (figure 2, figure S7, SI materials and methods).

Results

We found nine phenological regions (figure 1(a)) from the average monthly climatology of LST, NIR and QSCAT using *K*-means clustering (Seber 2004, Jain 2010)—an unsupervised measure to find similar features from multiple bands. The number of phenoregions was internally validated (figure S1) using both stability-based and variance-based statistical measures (Caliński and Harabasz 1974, Davies and Bouldin 1979, Tibshirani and Walther 2005) to ensure the clusters are well-separated (SI materials and methods). The clusters represent regions with (a) similar seasonal variations or phenology related to the amplitude and phase of observations (i.e. intra-annual variability),

and (b) similar landscape structure and biogeography related to annual mean values of observations (Steege *et al* 2013). We used principal component (PC) analysis (Hastie *et al* 2009) to visualize these two effects and found that the 1st and 2nd PC domain, containing 65% information of all observations, explain mainly variations in annual mean value (figure 1(b)). This was also confirmed using the clustering map of annual-mean-only data (figure S2) that explains 67% of the regional variations (table S1) in our clustered map (figure 1(a)). The seasonal effect (amplitude and phase) starts dominating the 3rd and 4th PC domain and explaining about 25% of all observations (figure 1(c)). Although the latter contribution is minor, it provides distinct spatial features (figure S2) highlighting the contribution of intra-annual variability in each pheno-region. The importance of this contribution can be readily demonstrated by statistically optimizing the number of clusters (figure S2).

Spatially, LST, NIR, and QSCAT all have different phases with rainfall or radiation seasonality (figure S3), indicating that climate alone cannot fully explain the geographical differences in vegetation seasonality. The seasonal variations of remote sensing observations appear to be significant even in the extremely wet regions of Amazonia (figure S4). The inclusion of these observations makes the detected seasonality patterns more spatially correlated and distinct with more than 70% of the cluster results predictable from nearby pixels (table S1). As our method never assumes any spatial autocorrelation, these results indicate the importance of spatial variations in amplitude, phase, and annual mean of remote sensing measurements in defining patterns of seasonality (figure S5).

Out of the nine pheno-regions, we delineated 7 large contiguous regions for detailed study of seasonality (boxes in figure 1(a)), and among them we selected three boxes with distinct seasonality for comparison: (1) the Southwestern Amazon (region 2) with ecologically dry seasons (EDS; monthly rainfall $\leqslant 100$ mm) extending 3–5 months, (2) the Central Amazon (region 3) with only 1 to 2 EDS months, and (3) the Eastern Guiana shield (region 6) with similar EDS as in region 2 but with a strong seasonal swing of radiation (figure S6). All three regions show decreasing canopy water content from QSCAT and increasing leaf temperature from LST during the dry season (figures 2(a)–(c)), but have obvious differences in NIR, with peaking in the middle of wet season in region 2 (figure 2(a)), about the end of dry season in region 3 (figure 2(b)), and to the middle of dry season in region 6 (figure 2(c)). The range of LST and the amplitude of QSCAT also vary from region to region. In Southwestern Amazonia, QSCAT and LST are strongly out of phase, with peak loss of canopy water content (drop in QSCAT) matching the maximum leaf temperature (increase in LST) during the middle to the end of dry season. In contrast, NIR peaks in wet season but start increasing from the middle of dry season as a response to deeper penetration of NIR signal and strong sensitivity to exposed understory vegetation. From Southwest to Northeast Amazonia, NIR's peak gradually shifts to the middle of dry season as radiation plays increasingly a dominant role in vegetation seasonality and promoting photosynthetic activity in dry season when light is abundant and water is still sufficient (low QSCAT amplitude). The region in Central Amazonia falls in between the two extremes with complex seasonality controlled by a combined water and light influence represented by the lagged behavior of QSCAT, LST with NIR.

These variations in observed vegetation phenology have an aggregate effect on the seasonality of GPP. Using upscaled GPP data as the reference (Beer *et al* 2010, Jung *et al* 2011), we found regional GPP seasonality being in phase with NIR during the dry season, remaining high in the wet season in agreement with QSCAT and/or LST, and strongly following the patterns of SIF data from the GOSAT (Frankenberg *et al* 2011, Lee *et al* 2013)—an independent measure of GPP directly linking to the photosynthetic activity (figures 2(d)–(f)). GPP peaks during the wet season in Southwest and dry season in Northeast regions of Amazonia respectively responding directly to water and radiation abundance.

These distinct patterns further confirm the heterogeneity of seasonality of forests of Amazonia related to regional variations of water and light constraints, directly addressing the question of whether Amazonian forests are water- or light-limited. We found two regions in Southern Amazonia (regions 1 and 2) with GPP peaks during the wet season (figure 2(d), figure S7); two regions in Central and Western Amazon (regions 3 and 4) showing rising GPP during the dry season (figure 2(e), figure S7); the region in Eastern Guiana shield (region 6) has GPP rising and peaking during the dry season (figure 2(f)); and the remaining two regions (regions 5 and 7) are less seasonal but showing two weak seasons within an annual cycle caused by lagged intensity of water and radiation (figures S7 and S8). The seasonal patterns of GPP are present in North–South and East–West gradient in all vegetation characteristics measured by the remote sensing data (figure S9). The overall agreement of upscaled GPP data with satellite observations to capture the large scale regional patterns of seasonality suggest that the satellite observations may be used to predict regional patterns of the carbon exchange seasonality in Amazonia. These regional patterns are extensive in size and internally heterogeneous in forest cover and landscape features, making the direct ground verification of GPP or vegetation seasonality difficult, unless through systematic and widespread measurements. However, similar patterns have been observed with spatially limited but comprehensive ground measurements of forest productivity, leaf fall and flushing, and seasonal carbon fluxes from the Global Ecosystem Monitoring network plots (del Aguila-Pasquel *et al* 2014, Araujo-Murakami *et al* 2014,

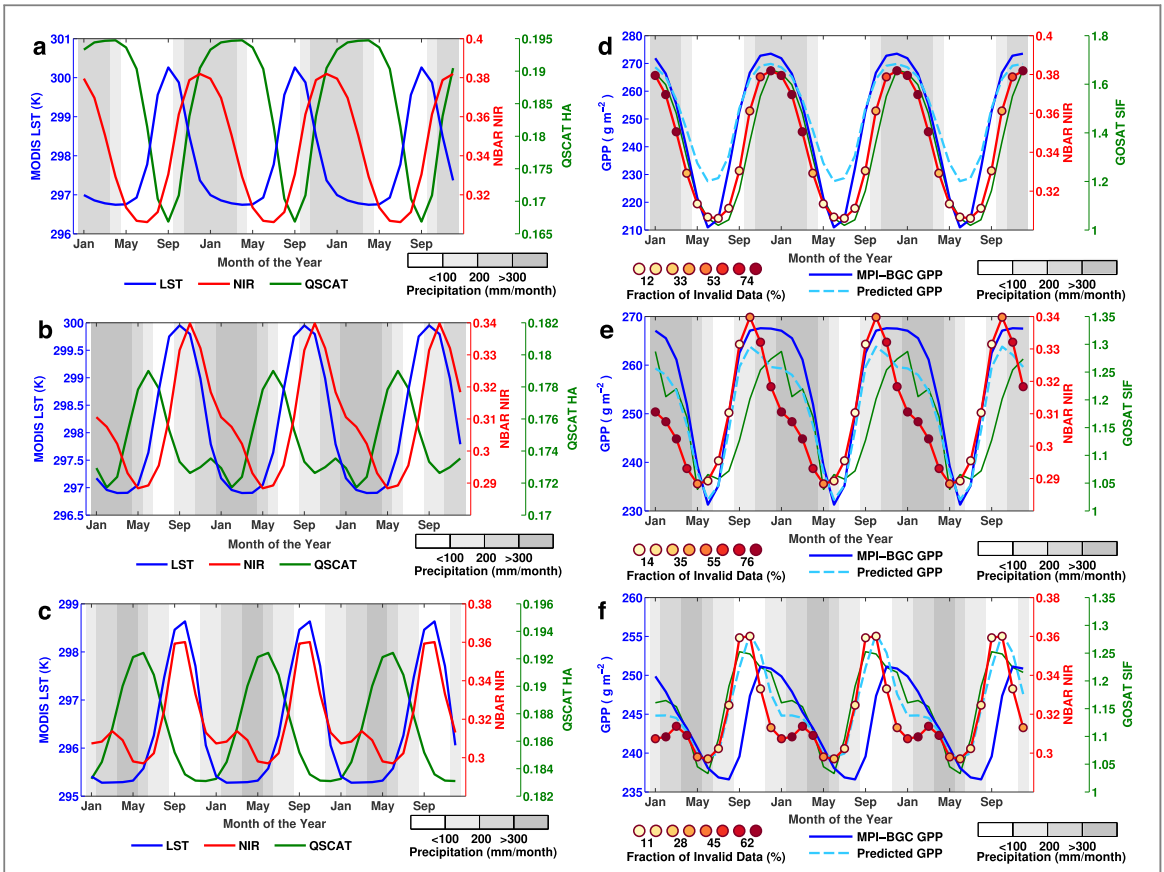

Figure 2. Time series of seasonality in selected regions. Left panels show the averaged seasonal cycles of LST, NIR and QSCAT data in (a) region 2, (b) region 3, and (c) region 6 defined from figure 1(a); right panels show the seasonal cycles of NIR, MPI-BGC GPP, GOSAT sun-induced chlorophyll fluorescence (SIF), and the predicted GPP curve (SI materials and methods) in (d) region 2, (e) region 3, and (f) region 6. The colored circles in the right panels denote the fraction of invalid data in each NIR observation period. Spatial averages in all regions take only pixels from the EBF class into calculation. Precipitation values are from the TRMM product (SI materials and methods). The annual cycle (January–December) is replicated 3 times for better demonstration.

Doughty *et al* 2014, Galbraith *et al* 2014, Malhi *et al* 2014), supporting satellite observed photosynthesis patterns related to the water and radiation variations across Amazonia (SI discussion).

Discussion and conclusions

The spatial heterogeneity in GPP seasonality cannot be explained by only a single vegetation variable. The canopy temperature and structure from LST has a nonlinear relationship with GPP (figure 3(a)), showing a steady increase until reaching a threshold and then followed by a gradual decline. This behavior agrees with observations showing an optimum range of temperature for forest photosynthesis (Berry and Bjorkman 1980, Wood *et al* 2012). GPP shows a strong sensitivity to water deficit as measured by QSCAT backscatter, but quickly decouples from water when forest canopy accumulates enough water and has no limitations for photosynthesis (figure 3(c)). Over some wet regions of Amazonia, GPP may even drop with increasing water content (regions 3, 4 and 6), pointing to low solar radiation or water-logged vegetation, both impairing photosynthetic activity (figure S10; SI discussion). Though regionally it appears to have tight negative correlation between canopy water and GPP, it may not truly reflect a causal relationship between them because of the small range of variations in the saturation zone of QSCAT (figure 3(c)), and the covariance with other variables such as NIR and LST. We found MODIS NIR being in phase and monotonically increasing with GPP over the Amazon basin (figure 3(b)), but also have large variations due to the heterogeneity of vegetation composition and seasonality, and potential presence of atmospheric effects during the wet season (figures 2(d)–(f)).

From the multi-sensor data analysis, we found a strong positive relation between NIR and GPP and SIF (figure S10) except in region 5 where there is very low seasonality and all vegetation variables including the relationship between GPP and SIF remain weak (figure S10). Vegetation seasonality captured by three remote sensing data (LST, QSCAT, NIR) together explain 60% of the GPP over the entire Amazon Basin with much larger explanatory significance in more seasonal regions. The variations around the mean in the relationship between the magnitude of GPP and remote sensing data are largely due to the heterogeneity of forest composition, canopy structure, and nutrient availability impacting forest carbon cycling

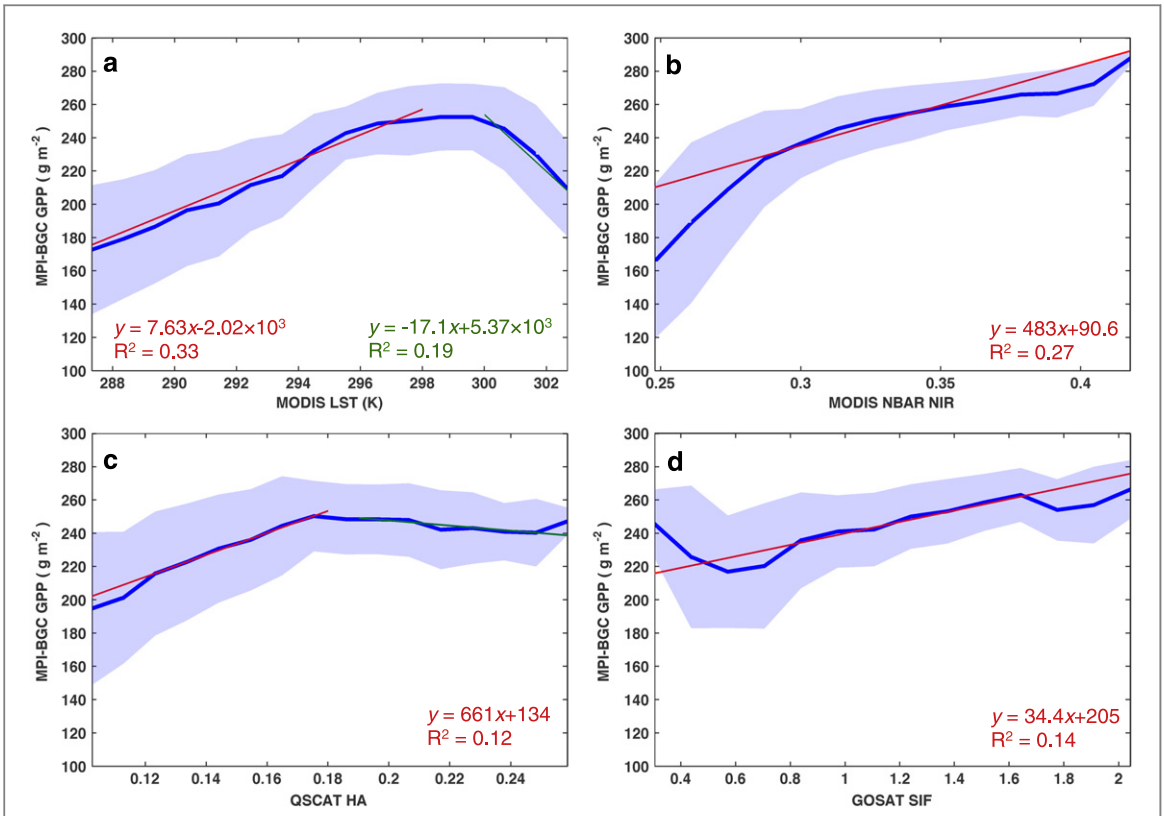

Figure 3. Relationships between GPP and remote sensing variables. (a) LST, (b) NIR, (c) QSCAT, and (d) GOSAT SIF. Blue line in each panel denotes the mean GPP varying with each variable, and the shaded area shows the variation of GPP with ±1 standard deviation. All observations were resampled to be the same resolution as MPI-BGC GPP (0.5° × 0.5°) using spatial average. The linear regressions were calculated from all pixels within the selected ranges (i.e. 2 selected ranges for LST: <298K and >300K; 1 selected range for QSCAT: <0.18; and the full range for NIR and SIF), and marked in red for the first selected range and green for the second selected range (LST only).

and exchange. We also expect the uncertainty in the benchmark GPP due to limited tower data in tropical regions may have contributed to the lack of correlation between GPP and satellite observations of forest canopy. Our results also show that the NDVI vegetation greenness index is not suitable for tropical seasonality analysis in terms of GPP variation (SI discussion).

In analyzing passive optical data (LST and NIR) over each region, we made sure that all regional patterns are extracted from a majority of the pixels in each region that are valid after careful data quality check (SI discussion). However, the atmospheric contamination from clouds and aerosols may still affect the surface retrievals due to small cumulus clouds within a pixel that cannot be readily detected by MODIS cloud detection tools (Koren *et al* 2008). With the presence of residual atmospheric effect in the pixels labeled as cloud-free, the spectral changes in the optical domain can be complicated. One could expect that NIR may either be elevated due to undetected clouds or reduced due to shadows. And LST, on the other hand, could be suppressed under persistent clouds. Even if we used the MODIS climatologically averaged data over 10 years with both geometric corrections and high quality flag filtering, and working with large area averages for clustering, the use and interpretation of these optical data in the tropical regions should still be treated with extreme caution. The large scale spectral variability of tropical forest due to canopy phenology makes it difficult to investigate whether the extent of changes in optical observations are due to physiological response of leaf fall and flushing, or the residual effect of small scale cloud contamination. A good example is the poor quality of optical data in the wet season, where we see the divergence between NIR and GPP explicitly presented in region 3 (figures 2(e)) and 4 (figure S7(b)). For seasonal changes of GPP in this period, it is necessary and essential to include the microwave data into the data analysis to compensate for the loss of optical data quality (SI discussion). The evaluation and uncertainty assessment of the optical data use in the tropical regions must be performed by using techniques that include airborne and *in situ* data.

A handful of flux tower measurements of GPP seasonality are the only ground-based resource existing in the Amazonian forests that are suitable for intercomparison with satellite observations. We selected 5 tropical forests sites in Amazonia and digitized the GPP curves from the research article of Restrepo-Coupe *et al* (2013) (figure 4). Results show that the *in situ* GPP curves are in phase with the NIR curves, particularly in the dry season and following the same regional patterns (figure 2). Though the magnitude of

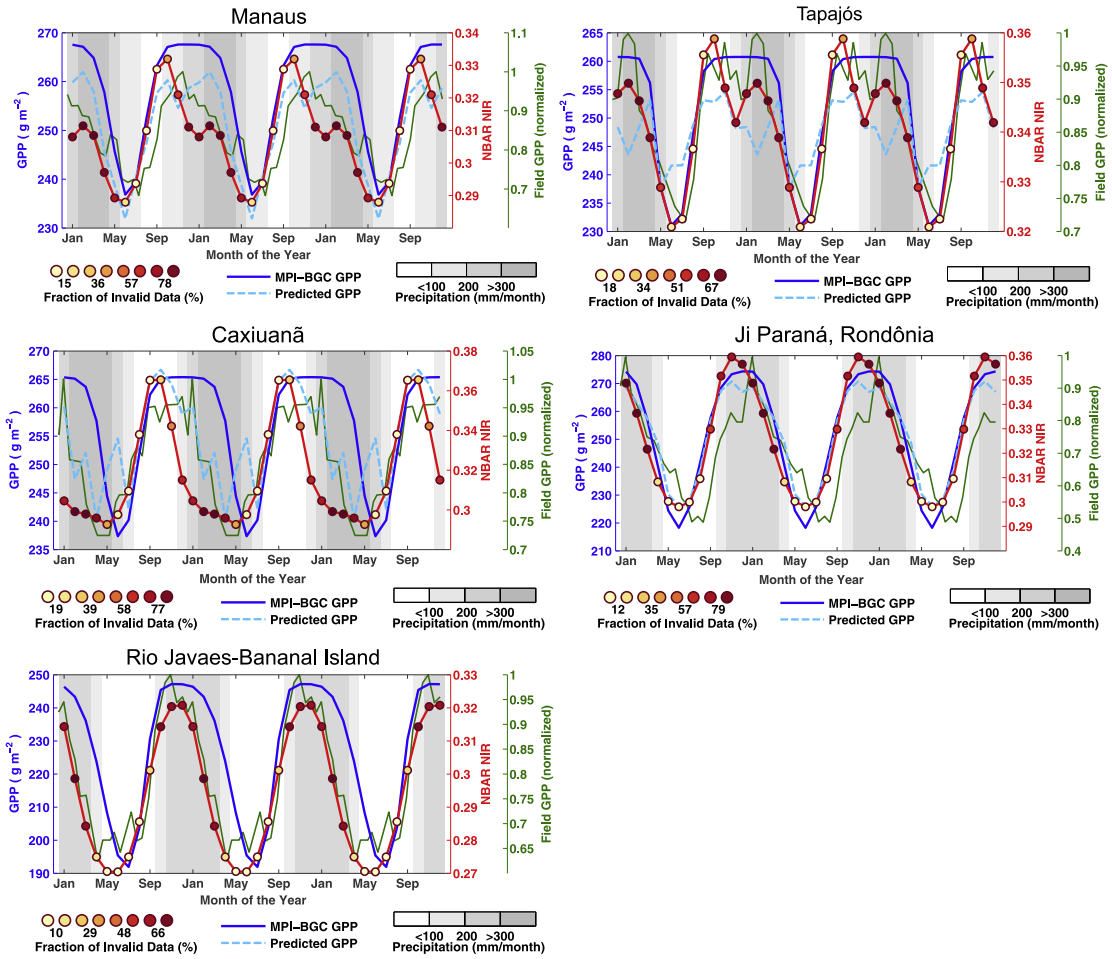

Figure 4. Time series of seasonality in flux tower sites. The displayed curves are the mean seasonal cycles of NIR, MPI-BGC GPP, field derived GPP, and the predicted GPP curve (SI Materials and Methods) in Manaus (2.61°S, 60.21°W), Tapajós (2.85°S, 54.97°W), Caxiuanã (1.72°S, 51.53°W), Ji Paraná, Rondônia (10.08°S, 61.93°W), and Rio Javaes-Bananal Island (9.82°S, 50.13°W). Field GPP was digitized from the GEP curves of figure 3 in Restrepo-Coupe *et al* (2013). The colored circles on the red lines denote the fraction of invalid data in each NIR observation period. Spatial averages in all regions take only pixels from the EBF class into calculation. Precipitation values are from the TRMM product (SI materials and methods). The annual cycle (January–December) is replicated three times for better demonstration. Reprinted from Restrepo-Coupe *et al* (2013), Copyright 2013, with permission from Elsevier.

GPP from *in situ* and gridded products are not comparable due to the normalized units used in *in situ* GPP, the MPI-BGC GPP are well in phase with the tower data, partially because they are essentially integrated in the MPI-BGC GPP benchmark data. However, the most interesting finding of the comparisons with the *in situ* data is the overall agreement with the regional pattern in each pheno-region that we defined purely from remote sensing data. Flux sites in Manaus, Tapajós, and Caxiuanã all show a rising GPP during the dry season with a peak at the end of dry season, consistent with their regional average represented by region 3 (figure 2(e)), while the other two tower sites in Ji Paraná and Rio Javaes-Bananal Island, belonging to the pheno-region 1, both exhibit GPP peaking during the middle of wet season and about 2 to 3 months later than the peak shown in region 3. These results, though limited in quantity, prove the validity of our pheno-region clusters and the general agreements between GPP and remote sensing observations of canopy characteristics. With more validation resources being available in the Amazonia (Galbraith *et al* 2014), the prediction strength of GPP seasonality is expected to be improved significantly.

The carbon exchange of tropical vegetation, whether light-controlled or water-limited, can vary not only in space, but also in time. The illustration using the average GPP response to different incoming radiation and precipitation (figure 5) conceptually shows that the flux tower sites located in different regions can respond to large variations in climate-driven seasonality. The São Gabriel da Cachoeira tower (Saleska *et al* 2009) in Northwestern Brazilian Amazon (monthly rainfall > 200 mm) has high GPP and less seasonal amplitude due to small changes in radiation and rainfall throughout the year (see region 5, figures S7 and S8). In contrast, the Ji Paraná tower site (Saleska *et al* 2009, Restrepo-Coupe *et al* 2013) in Southern Amazonia has enough radiation throughout the year (>200 Wm^{-2}) causing GPP varying strongly along the precipitation axis. In the case of the Central Amazon tower site located near the city of

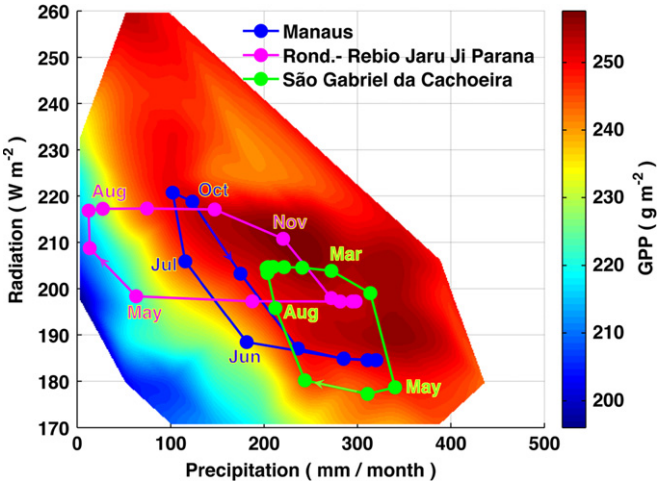

Figure 5. Relationship between estimated average GPP and climate variation in Amazonia. The GPP value is the average estimation of GPP predicted from the LST, NIR and QSCAT, given the condition of radiation and precipitation in each 1° box. Monthly total precipitation is from the TRMM product, and monthly average downward surface shortwave radiation is from the CERES product (SI materials and methods). The selected seasonal cycles were also plotted at locations where *insitu* measurements can be obtained from flux towers.

Manaus (Restrepo-Coupe *et al* 2013), GPP has a moderate seasonal variation driven by a hybrid effect of rainfall and radiation causing the GPP increase from October to May rainy season, a short drop in May and June with the decline of rainfall, and a sharp increase from late June to late September from increased radiation.

Using more accurate estimation of chlorophyll fluorescence from GOSAT, we show that while Amazon forests as a whole retain high productivity during the year, there are distinct regional patterns of seasonality. These patterns are potentially driven by variations in forest species, structure, nutrient availability, and climate variations over Amazonia, creating complex mechanisms to regulate photosynthetic carbon assimilation through water and light availability and dynamic stomatal responses (Lee *et al* 2013). Contrary to recent findings, our analysis of multiple satellite observations along with ground measurements of leaf dynamics (Galbraith *et al* 2014) indicate that Amazonia does not maintain a consistent canopy throughout the year, and variations of carbon exchange in Amazonia are reflected by potential changes of top canopy structure regionally during dry and wet seasons. Regional differences in vegetation seasonality in the Amazon basin also demand further research and measurements to understand and quantify the vulnerability of each pheno-region to future changes of climate and seasonality. A phase shift off the stable pattern of seasonality these forests could mean increased risks of ecosystem stress and disturbance, water loss, and carbon release, which can have significant impacts at the global scale given the huge amount of carbon stored in the Amazon forests.

Acknowledgments

This work was funded by NASA Earth Science Division. We thank NSIDC, BYU, NASA MODIS Project, NASA GSFC, and CERES science team for making their data available. The authors thank C J Tucker and J E Pinzon for providing the newer version of AVHRR NDVI. We also thank M Jung for the upscaled GPP data set available at the MPI-BGC data portal.

References

Araujo-Murakami A *et al* 2014 The productivity, allocation and cycling of carbon in forests at the dry margin of the Amazon forest in Bolivia *Plant Ecol. Divers.* **7** 55–69

Baker I T, Prihodko L, Denning A S, Goulden M, Miller S and da Rocha H R 2008 Seasonal drought stress in the Amazon: Reconciling models and observations *J. Geophys. Res. Biogeosciences* **113** G00B01

Beer C *et al* 2010 Terrestrial gross carbon dioxide uptake: global distribution and covariation with climate *Science* **329** 834–8

Beer C, Reichstein M, Ciais P, Farquhar G D and Papale D 2007 Mean annual GPP of Europe derived from its water balance *Geophys. Res. Lett.* **34** L05401

Berry J and Bjorkman O 1980 Photosynthetic response and adaptation to temperature in higher plants *Annu. Rev. Plant Physiol.* **31** 491–543

Breiman L 2001 Random forests *Mach. Learn.* **45** 5–32

Caliński T and Harabasz J 1974 A dendrite method for cluster analysis *Commun. Stat.* **3** 1–27

Clark D A 2004 Sources or sinks? the responses of tropical forests to current and future climate and atmospheric composition *Phil. Trans. R. Soc.* B **359** 477–91

Davies D L and Bouldin D W 1979 A cluster separation measure *IEEE Trans. Pattern Anal. Mach. Intell.* **1** 224–7

Del Aguila-Pasquel J *et al* 2014 The seasonal cycle of productivity, metabolism and carbon dynamics in a wet aseasonal forest in North-West Amazonia (Iquitos, Peru) *Plant Ecol. Divers.* **7** 71–83

Doughty C E *et al* 2014 The production, allocation and cycling of carbon in a forest on fertile *terra preta* soil in Eastern

Amazonia compared with a forest on adjacent infertile soil *Plant Ecol. Divers.* **7** 41–53
Eklundh L and Jönsson P 2011 *TIMESAT 3.1 Software Manual* (Sweden: Lund University)
Fischer R, Armstrong A, Shugart H H and Huth A 2014 Simulating the impacts of reduced rainfall on carbon stocks and net ecosystem exchange in a tropical forest *Environ. Model. Softw.* **52** 200–6
Frankenberg C *et al* 2011 New global observations of the terrestrial carbon cycle from GOSAT: patterns of plant fluorescence with gross primary productivity *Geophys. Res. Lett.* **38** L17706
Frolking S, Milliman T, Palace M, Wisser D, Lammers R and Fahnestock M 2011 Tropical forest backscatter anomaly evident in seawinds scatterometer morning overpass data during 2005 drought in Amazonia *Remote Sens. Environ.* **115** 897–907
Fu R *et al* 2013 Increased dry-season length over Southern Amazonia in recent decades and its implication for future climate projection *Proc. Natl Acad. Sci.* **110** 18110–5
Galbraith D, Malhi Y, Aragão L and Baker T 2014 The ecosystem dynamics of Amazonian and Andean forests *Plant Ecol. Divers.* **7** 1–6
Hashimoto H, Wang W, Milesi C, White M A, Ganguly S, Gamo M, Hirata R, Myneni R B and Nemani R R 2012 Exploring simple algorithms for estimating gross primary production in forested areas from satellite data *Remote Sens.* **4** 303–26
Hastie T, Tibshirani R and Friedman J 2009 Unsupervised learning *The Elements of Statistical Learning* (*Springer Series in Statistics*) (New York: Springer) pp 485–585
Hilker T, Lyapustin A I, Tucker C J, Hall F G, Myneni R B, Wang Y, Bi J, Moura Y M de and Sellers P J 2014 Vegetation dynamics and rainfall sensitivity of the Amazon *Proc. Natl Acad. Sci.* **111** 16041–6
Huete A R, Didan K, Shimabukuro Y E, Ratana P, Saleska S R, Hutyra L R, Yang W, Nemani R R and Myneni R 2006 Amazon rainforests green-up with sunlight in dry season *Geophys. Res. Lett.* **33** L06405
Huntingford C *et al* 2013 Simulated resilience of tropical rainforests to CO_2-induced climate change *Nat. Geosci.* **6** 268–73
Hutyra L R, Munger J W, Saleska S R, Gottlieb E, Daube B C, Dunn A L, Amaral D F, de Camargo P B and Wofsy S C 2007 Seasonal controls on the exchange of carbon and water in an Amazonian rain forest *J. Geophys. Res. Biogeosciences* **112** G03008
Jain A K 2010 Data clustering: 50 years beyond *K*-means *Pattern Recognit. Lett.* **31** 651–66
Jung M *et al* 2011 Global patterns of land-atmosphere fluxes of carbon dioxide, latent heat, and sensible heat derived from eddy covariance, satellite, and meteorological observations *J. Geophys. Res. Biogeosciences* **116** G00J07
Jönsson P and Eklundh L 2002 Seasonality extraction by function fitting to time-series of satellite sensor data *IEEE Trans. Geosci. Remote Sens.* **40** 1824–32
Jönsson P and Eklundh L 2004 TIMESAT—a program for analyzing time-series of satellite sensor data *Comput. Geosci.* **30** 833–45
Kim Y, Knox R G, Longo M, Medvigy D, Hutyra L R, Pyle E H, Wofsy S C, Bras R L and Moorcroft P R 2012 Seasonal carbon dynamics and water fluxes in an Amazon rainforest *Glob. Change Biol.* **18** 1322–34
Knyazikhin Y *et al* 2013 Hyperspectral remote sensing of foliar nitrogen content *Proc. Natl Acad. Sci.* **110** E185–92
Koren I, Oreopoulos L, Feingold G, Remer L A and Altaratz O 2008 How small is a small cloud? *Atmos. Chem. Phys.* **8** 3855–64
Lee J-E *et al* 2013 Forest productivity and water stress in Amazonia: observations from GOSAT chlorophyll fluorescence *Proc. R. Soc.* B **280** 20130171
Maeda E E, Heiskanen J, Aragão L E O C and Rinne J 2014 Can MODIS EVI monitor ecosystem productivity in the Amazon rainforest? *Geophys. Res. Lett.* **41** 2014GL061535
Malhi Y *et al* 2014 The productivity, metabolism and carbon cycle of two lowland tropical forest plots in South-Western Amazonia, Peru *Plant Ecol. Divers.* **7** 85–105
Malhi Y, Saatchi S, Girardin C and Aragão L E O C 2009 The production, storage, and flow of carbon in Amazonian forests *Amazonia and Global Change* ed M Keller, M Bustamante, J Gash and P S Dias (Washington: American Geophysical Union) pp 355–72
Monteith J L 1972 Solar radiation and productivity in tropical ecosystems *J. Appl. Ecol.* **9** 747–66
Morton D C, Nagol J, Carabajal C C, Rosette J, Palace M, Cook B D, Vermote E F, Harding D J and North P R J 2014 Amazon forests maintain consistent canopy structure and greenness during the dry season *Nature* **506** 221–4
Myneni R B *et al* 2007 Large seasonal swings in leaf area of Amazon rainforests *Proc. Natl Acad. Sci.* **104** 4820–3
Restrepo-Coupe N *et al* 2013 What drives the seasonality of photosynthesis across the Amazon basin? a cross-site analysis of eddy flux tower measurements from the Brasil flux network *Agric. For. Meteorol.* **182–3** 128–44
Rowland L, Malhi Y, Silva-Espejo J E, Farfán-Amézquita F, Halladay K, Doughty C E, Meir P and Phillips O L 2014 The sensitivity of wood production to seasonal and interannual variations in climate in a lowland Amazonian rainforest *Oecologia* **174** 295–306
Running S W, Nemani R R, Heinsch F A, Zhao M, Reeves M and Hashimoto H 2004 A continuous satellite-derived measure of global terrestrial primary production *BioScience* **54** 547
Saatchi S, Asefi-Najafabady S, Malhi Y, Aragão L E O C, Anderson L O, Myneni R B and Nemani R 2013 Persistent effects of a severe drought on Amazonian forest canopy *Proc. Natl Acad. Sci.* **110** 565–70
Saleska S, Da Rocha H, Kruijt B and Nobre A 2009 Ecosystem carbon fluxes and Amazonian forest metabolism *Amazonia and Global Change* ed M Keller, M Bustamante, J Gash and P S Dias (Washington : American Geophysical Union) pp 389–407
Saleska S R *et al* 2003 Carbon in Amazon forests: unexpected seasonal fluxes and disturbance-induced losses *Science* **302** 1554–7
Samanta A, Ganguly S, Hashimoto H, Devadiga S, Vermote E, Knyazikhin Y, Nemani R R and Myneni R B 2010 Amazon forests did not green-up during the 2005 drought *Geophys. Res. Lett.* **37** L05401
Samanta A, Knyazikhin Y, Xu L, Dickinson R E, Fu R, Costa M H, Saatchi S S, Nemani R R and Myneni R B 2012 Seasonal changes in leaf area of Amazon forests from leaf flushing and abscission *J. Geophys. Res.* **117** L05401
Schaaf C B *et al* 2002 First operational BRDF, albedo nadir reflectance products from MODIS *Remote Sens. Environ.* **83** 135–48
Schaaf C B, Liu J, Gao F and Strahler A H 2011 Aqua and terra MODIS albedo and reflectance anisotropy products *Land Remote Sensing and Global Environmental Change Remote Sensing and Digital Image Processing* ed B Ramachandran, C O Justice and M J Abrams (New York : Springer) pp 549–61
Schimel D, Pavlick R, Fisher J B, Asner G P, Saatchi S, Townsend P, Miller C, Frankenberg C, Hibbard K and Cox P 2014 Observing terrestrial ecosystems and the carbon cycle from space *Glob. Change Biol.* **21** 1762–76
Seber G A F 2004 *Multivariate Observations* (Hoboken, N.J.: Interscience)
Silva F B, Shimabukuro Y E, Aragão L E O C, Anderson, Pereira, Cardozo and Arai 2013 Large-scale heterogeneity of Amazonian phenology revealed from 26 year long AVHRR/NDVI time-series *Environ. Res. Lett.* **8** 024011
Sims D A *et al* 2008 A new model of gross primary productivity for North American ecosystems based solely on the enhanced vegetation index and land surface temperature from MODIS *Remote Sens. Environ.* **112** 1633–46
Steege H T *et al* 2013 Hyperdominance in the Amazonian tree flora *Science* **342** 1243092
Tibshirani R and Walther G 2005 Cluster validation by prediction strength *J. Comput. Graph. Stat.* **14** 511–28
Vourlitis G L, de Souza N J, Filho N P, Hoeger W, Raiter F, Biudes M S, Arruda J C, Capistrano V B, Brito de Faria J L and

de Almeida L F 2005 The sensitivity of Diel CO_2 and H_2O vapor exchange of a tropical transitional forest to seasonal variation in meteorology and water availability *Earth Interact.* **9** 1–23

Wan Z 2008 New refinements and validation of the MODIS land-surface temperature/emissivity products *Remote Sens. Environ.* **112** 59–74

White M A, Hoffman F, Hargrove W W and Nemani R R 2005 A global framework for monitoring phenological responses to climate change *Geophys. Res. Lett.* **32** L04705

Wood T E, Cavaleri M A and Reed S C 2012 Tropical forest carbon balance in a warmer world: a critical review spanning microbial- to ecosystem-scale processes *Biol. Rev.* **87** 912–27